

Computer simulation of the isomerization mechanism and spectral characteristics of spiro[1,3,4]oxadiazines*

V. I. Minkin and A. A. Starikova*

Institute of Physical and Organic Chemistry, Southern Federal University,
194/2 prosp. Stachki, 344090 Rostov-on-Don, Russian Federation.

E-mail: alstar@ipoc.sfedu.ru

Structural and spectral characteristics of spiro[1,3,4]oxadiazines were calculated by density functional theory method (B3LYP/6-311++G(d,p)). It is shown that a fundamental difference of spirooxadiazines from known spirocyclic compounds is that the ring-opened form is more energetically favorable (by 4.9 kcal mol⁻¹) compared to the ring-closed one. The closeness between the total energies of closed and open forms of spirooxadiazines suggests all isomers to coexist in solution. The intramolecular rearrangements of compounds under study associated with bond cleavage—formation are accompanied by overcoming of lower-energy barriers than those in the case of analogous spiropyrans and spiroxazines. The calculated electronic spectra (TD DFT) and overlapping absorption band maxima of the closed and open spirooxadiazine forms suggest a low probability of photoinitiated ring opening—closure in this compound.

Key words: quantum chemical simulation, spirocyclic compounds, spiro[1,3,4]oxadiazine, isomerization mechanism, spectral characteristics, density functional theory, B3LYP functional.

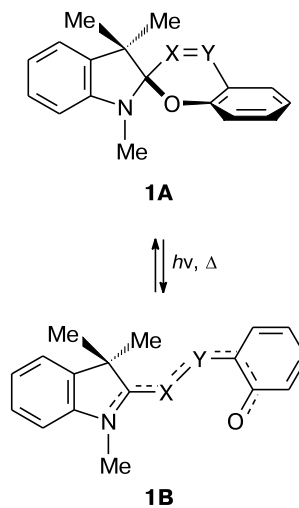
Spirocyclic compounds are unique molecular systems capable of undergoing photoinitiated changes in the physicochemical characteristics due to the equilibrium between the ring-closed usually colorless and ring-opened (merocyanine) colored forms. These compounds have found application as supports for high-capacity data recording optical devices, photochromic ophthalmologic lens, and high-sensitivity heavy metal sensors. They are expected to be used in the design of new-type molecular switches.^{1,2}

The most studied classes of spiro compounds **1** are spiropyrans (SPP, X = Y = CH) and spiroxazines (SPO, X = CH, Y = N) (Scheme 1); monographs^{3–5} and reviews^{6–10} are dedicated to the study of their structures, spectral properties, and photochromism. At the same time, the surprising thing is that there is no data on other type of potentially photochromic molecules, *i.e.*, spiro[1,3,4]-oxadiazines **1** (SPOD, X = Y = N) for which the equilibrium between the closed and open forms, as well as exhibition of photochromic properties are quite possible. The presence of one more photoisomerizable azo group can enrich considerably the photochromic properties of SPODs.

In the literature on the spirocyclic systems **1**, there is only superficial mention³ about unsuccessful attempts to synthesize SPODs. The possible reasons for difficulties in

* Dedicated to the Academician of the Russian Academy of Sciences N. S. Zefirov on the occasion of his 80th birthday.

Scheme 1



X, Y = CH, N

preparation of these compounds can be due to the thermodynamic instability of one or both isomeric forms of SPODs and the absence of data on their presumptive photochromic properties can be due to an insufficient spectral contrast of photoisomers. The aim of the present work is to assess the above-mentioned possibilities, to predict properties of SPODs, and to compare mechanism of their intramolecular rearrangements with the data obtained for

SPPs and SPOs using the results from quantum chemical calculations of structures 2–37.

Calculation Procedure

Quantum chemical calculations were performed in the Gaussian 03 program¹¹ by density functional theory (DFT)¹² method using B3LYP functional¹³ and 6-311++G(d,p) basis set. Earlier, we have shown that this approach reproduces correctly the energy characteristics of the tautomeric equilibrium between isomeric forms of spiro compounds.^{14–16} Stationary points on the potential energy surface (PES) were localized by full geometry optimization of molecular structures followed by calculation of force constants. The structures corresponding to the energy minima on the PES were determined by the method of steepest descent

(gradient motion) from the saddle point to the neighbor stationary point (saddle or minimum).¹⁷ Nonspecific solvation (acetonitrile) was taken into account in terms of continuum approach (IEFPCM).¹⁸ For compounds under study, the first twenty electron transitions were calculated by TD (time-dependent) DFT (B3LYP/6-311++G(d,p)). Graphical images of molecular structures were obtained using the ChemCraft program.¹⁹

Results and Discussion

Calculations of the closed forms of **2**, **10**, and **18** of basic spirocyclic compounds predict the close geometric characteristics of their spiro sites (Fig. 1). An exception is the C–N bond lengths which in SPODs are by 0.02–0.03 Å shorter than those in known spiro compounds.

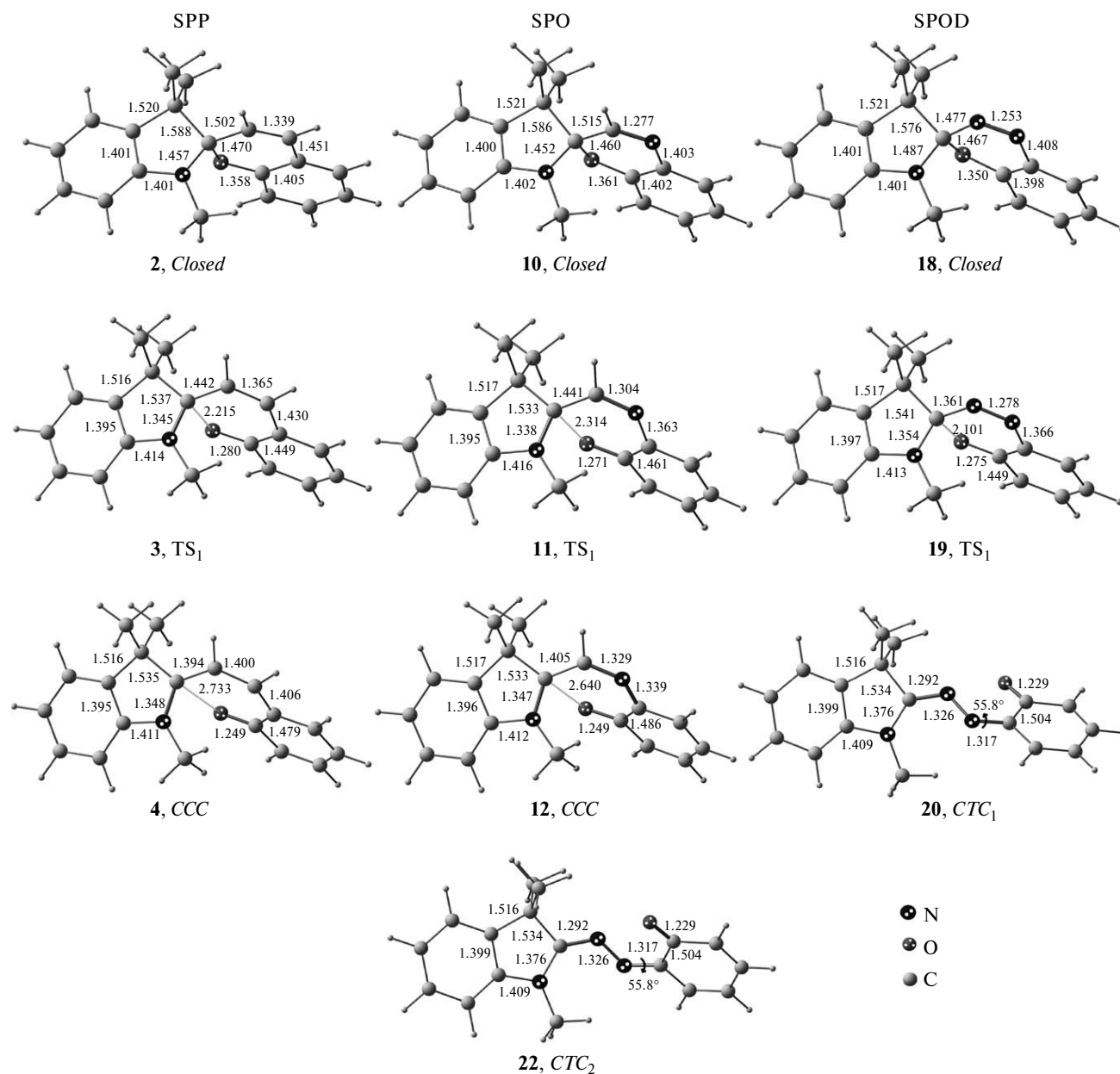


Fig. 1. DFT/B3LYP/6-311++G(d,p)-calculated geometric characteristics of the structures of SPPs **2**–**4**, SPOs **10**–**12**, and SPODs **18**–**20** and **22**. Here and in Figs 2, 3, and 6, the bond lengths are given Å.

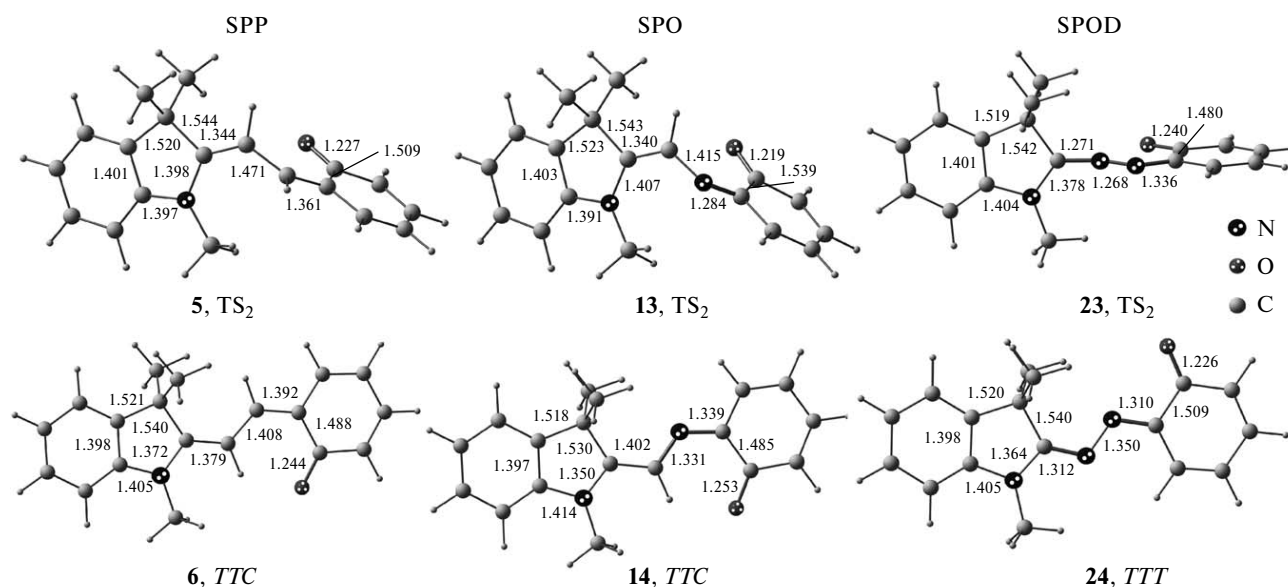


Fig. 2. DFT/B3LYP/6-311++G(d,p)-calculated geometric characteristics of the structures of SPPs **5** and **6**, SPOs **13** and **14**, and SPODs **23** and **24**.

The geometry analysis of transition states (TS) corresponding to spiro ring opening (see Fig. 1, structures **3**, **11**, and **19**) suggests a reduction in the distance between the C spiro

atom and the O atom in SPODs to ~ 2.1 Å; this distance for SPPs and SPOs is ~ 2.2 and ~ 2.3 Å, respectively.

Table 1. DFT/B3LYP/6-311++G(d,p)-calculated relative energies (kcal mol⁻¹) without (ΔE) and with taking into account the zero-point harmonic vibration energies (ΔE_{ZPE}) for structures **2**–**26**

Structure	Gas phase		Solution (IEFPCM, MeCN)	
	ΔE	ΔE_{ZPE}	ΔE	ΔE_{ZPE}
2 , Closed	0.0	0.0	0.0	0.0
3 , TS ₁	15.1	14.0	12.8	11.8
4 , CCC	12.5	11.7	9.4	8.7
5 , TS ₂	26.2	23.7	24.2	21.6
6 , TTC	5.5	4.6	0.6	-0.1
7 , TTT	6.8	5.8	6.9	5.4
8 , CTC	7.8	7.1	2.5	1.9
9 , CTT	8.0	7.2	6.9	5.4
10 , Closed	0.0	0.0	0.0	0.0
11 , TS ₁	19.1	17.7	15.9	14.6
12 , CCC	18.3	16.9	21.5	20.3
13 , TS ₂	31.7	28.8	30.4	27.5
14 , TTC	6.2	4.9	3.0	1.7
15 , TTT	11.7	10.1	1.0	0.1
16 , CTC	7.1	5.9	4.3	3.0
17 , CTT	11.1	9.5	2.5	1.9
18 , Closed	3.9	4.9	6.1	7.2
19 , TS ₁	13.9	13.6	15.1	14.9
20 , CTC ₁	4.9	4.7	5.9	5.6
21 , TS _{CTC}	6.8	6.5	7.4	7.0
22 , CTC ₂	4.9	4.7	5.9	5.6
23 , TS ₂	11.7	10.8	11.6	10.8
24 , TTT	0.0	0.0	0.0	0.0
25 , CTT	2.2	2.1	8.5	8.5
26 , TTC	2.6	2.5	2.9	3.1

The gradient descent from TSs **3** and **11** showed that opening of SPP and SPO rings results in the formation of *cis* structures (**4** and **12**, respectively). The analogous calculation of SPOD leads to structure **20** whose conformation can be classified as *cis*–*trans*–*cis* (CTC). Consequently, no isomer corresponding to the CCC form of SPOD exists, which is due to the stereochemical nonrigidity of the N–N fragment.

Cis–*trans* isomerization of the ring-opened forms of compounds under consideration is realized through TSs **5**, **13**, and **23** (Fig. 2). The distinctive feature of TS **23** is a perpendicular arrangement of the ring-opened part of the molecule relative to the plane of the indoline fragment.

In accordance with the literature data,^{20–22} calculations suggest the energy preference of *trans*–*trans*–*cis* (TTT) isomers **6** and **14** in the open forms of SPP and SPO and, in the case of SPOD, the *trans*–*trans*–*trans* (TTT) isomer **24** is more stable (Tables 1 and 2, see Fig. 2). Other open isomers of experimentally studied SPPs and SPOs are also characterized by a planar structure and destabilized by 5–10 kcal mol⁻¹ relative to the closed forms (see Table 1 and Fig. 3). The main difference of SPOD

Table 2. Absolute total energies (au) without (E_{tot}) and with taking into account the zero-point harmonic vibration energies ($E_{\text{tot, ZPE}}$) for structures **2**, **10**, and **24**

Structure	Gas phase		Solution (IEFPCM, MeCN)	
	E_{tot}	$E_{\text{tot, ZPE}}$	E_{tot}	$E_{\text{tot, ZPE}}$
2	-865.6527	-865.32101	-865.65671	-865.32533
10	-881.69390	-881.37380	-881.69901	-881.37920
24	-897.71145	-897.40550	-897.72143	-897.41568

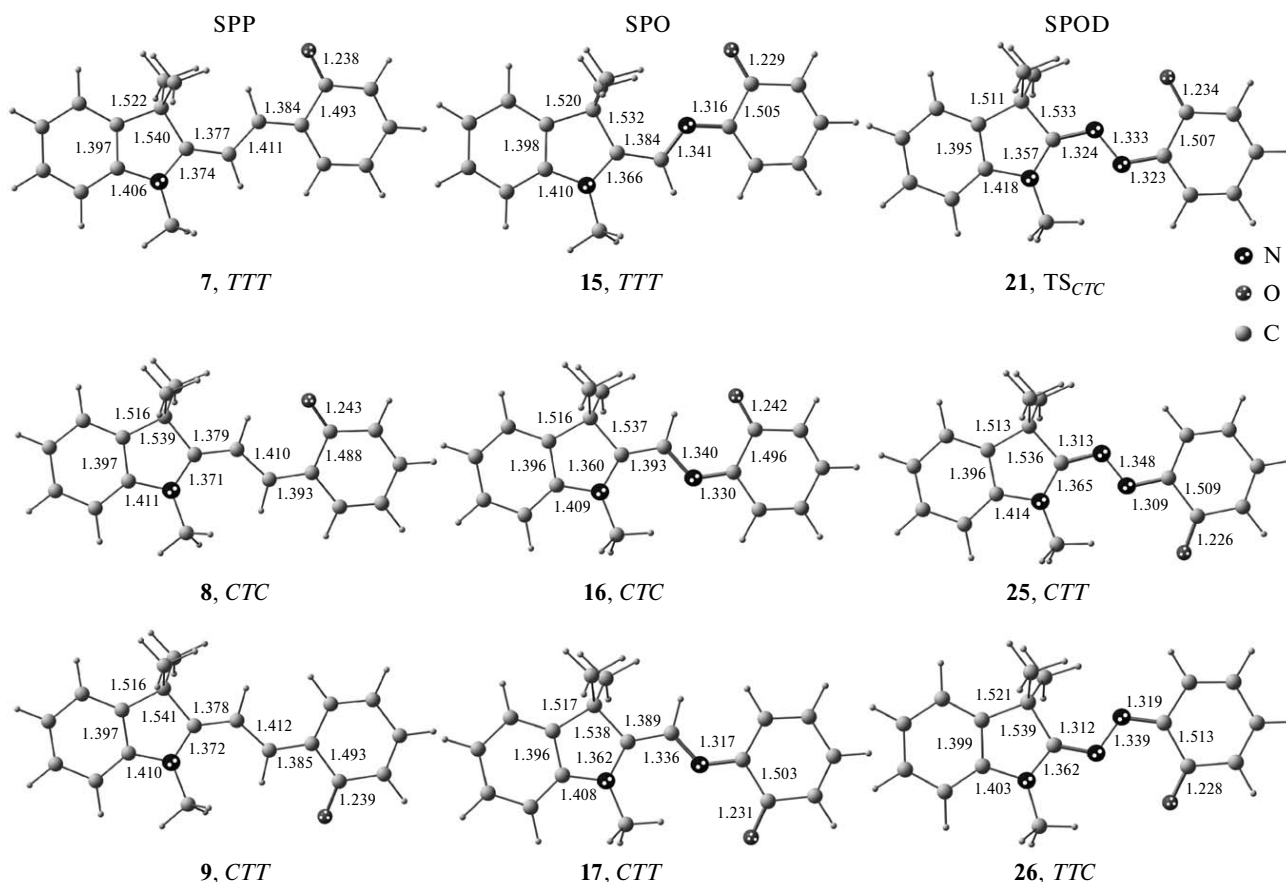


Fig. 3. DFT/B3LYP/6-311++G(d,p)-calculated geometric characteristics of the structures of SPPs 7–9, SPOs 15–17, and SPODs 21, 25, and 26.

from SPP and SPO is that the ring-opened form is energetically more preferable (by $4.9 \text{ kcal mol}^{-1}$) with regard to the ring-closed one.

Based on the data obtained, we simulated a mechanism of thermal ring opening of SPPs, SPOs, (Fig 4), and SPODs (Fig. 5). It follows from the energy profile of thermal isomerization of SPP shown in Fig. 4 that the closed form **2** is the ground state. The *TTC* structure **6** corresponding to the most stable ring-opened isomer is by

$4.6 \text{ kcal mol}^{-1}$ less stable than the closed form **2**. Spiro ring opening is accompanied by overcoming an energy barrier of $14.0 \text{ kcal mol}^{-1}$ and transition into the *cis* ring-opened *CCC* form **4** destabilized by $11.7 \text{ kcal mol}^{-1}$ relative to the closed form **2**. The rate-limiting step of the reaction under study is transition between the *cis* and *trans* forms. *TS 5* corresponding to this process is destabilized by $23.7 \text{ kcal mol}^{-1}$ with regard to the most stable form **2**. Consideration of the nonspecific solvation results in that

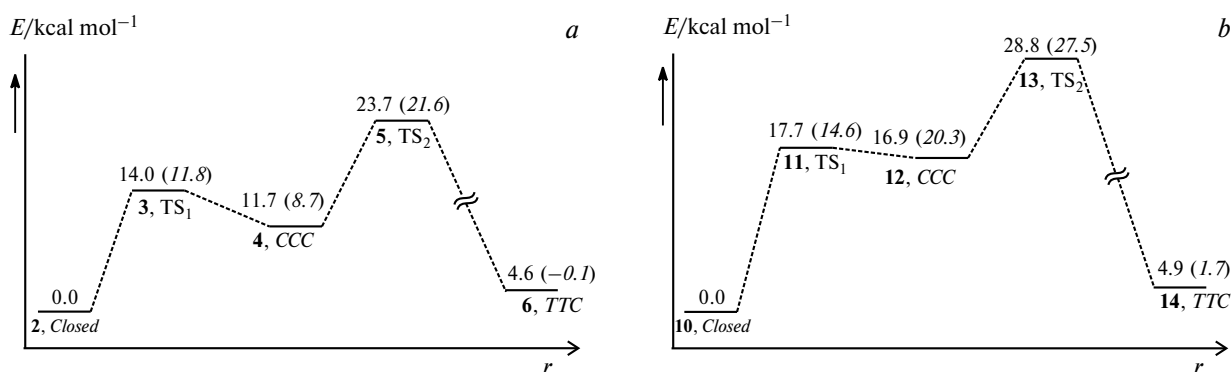


Fig. 4. Energy diagrams for thermal ring opening of SPP (a) and SPO (b) according to the DFT/B3LYP/6-311++G(d,p) calculation data. Here and in Fig. 5, the energies taking into account the nonspecific solvation (IEFPCM, MeCN) are given in parentheses; r is the reaction coordinate.

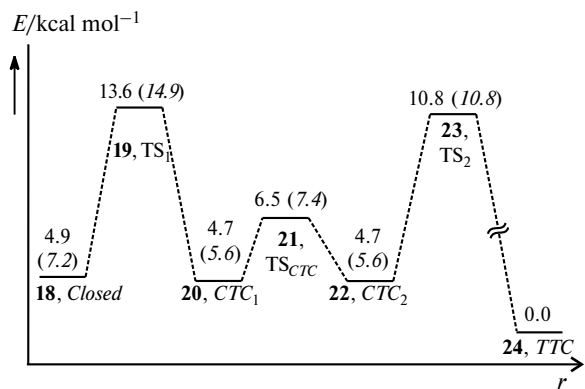


Fig. 5. Energy diagram for thermal ring opening of SPOD according to the DFT/B3LYP/6-311++G(d,p) calculation data.

the energy differences between the closed and open forms become closer and the energy barrier of the process under study decreases to 21.6 kcal mol⁻¹.

The mechanism of ring opening of SPO shown in Fig. 4, *b* generally coincides with that predicted for SPP, except for the increase in the energy of the CCC isomer **12** upon taking into account the nonspecific solvation. Calculations of the main pathway regions of thermal isomerization of SPP agrees well with the data from the theoretical studies performed earlier.^{23,24}

The scheme for thermal opening of the SPOD ring is shown in Fig. 5. The ground state of this compound is the ring-opened *TTT* form **24** which is by 4.9 kcal mol⁻¹ more stable than the closed form **18**. The reaction requires significantly lower energy costs compared to the above-considered compounds, which, taking into account the closeness between the total energies of the closed form **18** and the ring-opened SPOD forms **20**, **22**, and **24–26**, predicts the coexistence of all isomers in solution. On the ring opening pathway of the compound under study, we detected a low-energy TS **21**, TS_{CTC} between two nonplanar CTC isomers (**20**, CTC₁ and **22**, CTC₂). The effect of sol-

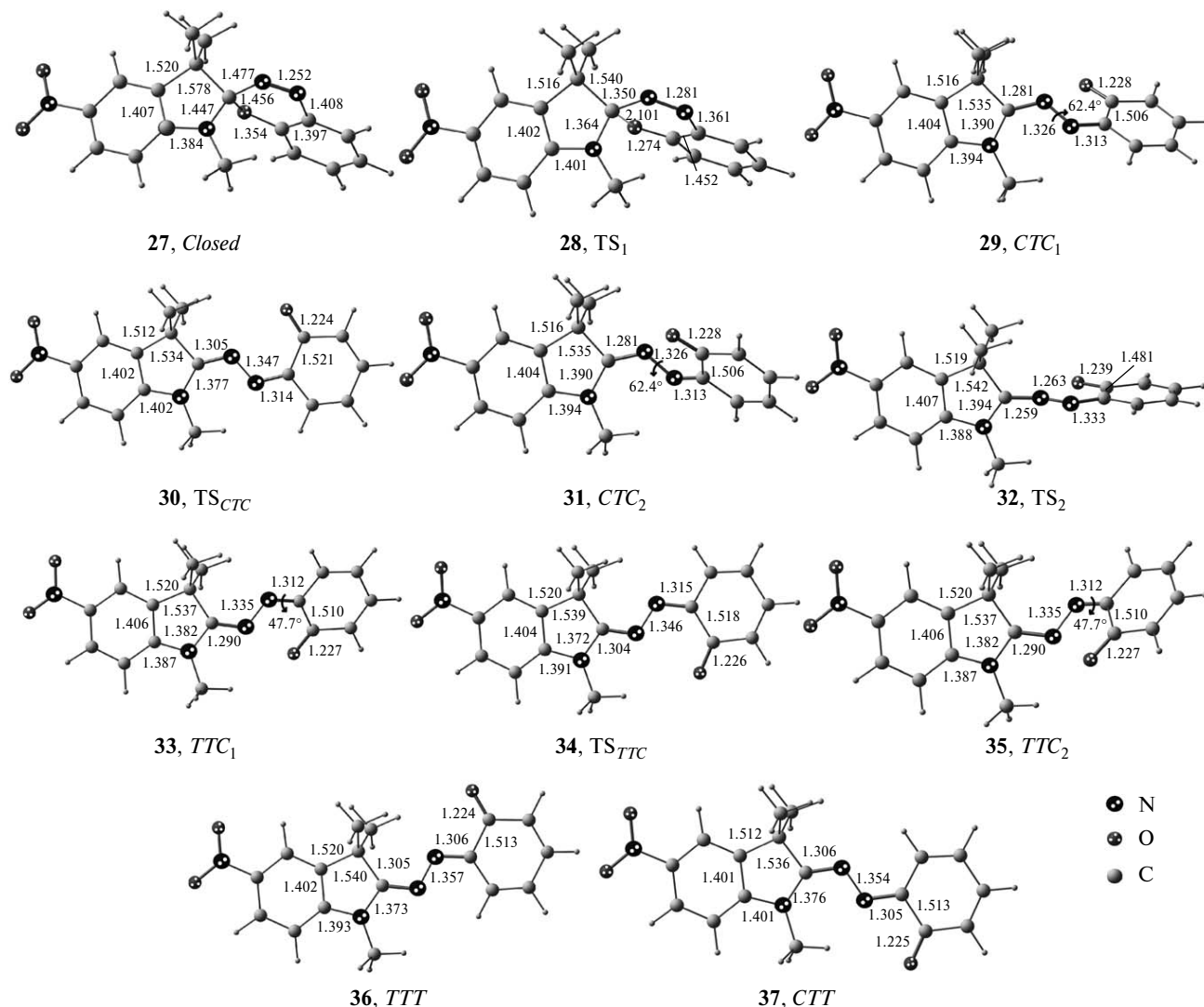


Fig. 6. DFT/B3LYP/6-311++G(d,p)-calculated geometric characteristics of the SPOD structures 27–37.

vation on isomerization of the SPOD results in insignificant increases in the energy barrier of the process under study and in the energy difference between the closed and most stable ring-opened forms.

Insertion of electron-withdrawing groups to the 5 position of the indoline fragment of SPP and SPO is known to decrease the relative stability of the merocyanine isomer.⁵ In order to search for a SPOD with a ring-closed form being the most stable state, a compound containing the nitro group in the indoline moiety was studied (Fig. 6).

As it follows from the data shown in Fig. 6 and given in Table 3, insertion of the NO₂ group decreases the energy difference between the most stable *TTT* isomer **36** and the closed form **27** to 2.5 kcal mol⁻¹, which allows one to expect the simultaneous presence of ring-closed and -opened forms in solution. **TS 28** corresponding to ring opening is close by the relative energy and the geometry characteristics to the analogous structure **19** of the unsubstituted SPOD (see Fig. 1 and Table 1). The planar *CTC* structure **30** is a TS between isomers **29**, *CTC*₁ and **31**, *CTC*₂. A significant difference of the NO₂-substituted SPOD from the unsubstituted one is that the *TTC* structure **34** corresponds to the transition state (**TS**_{*TTC*}) the gradient descent from which results in two isomers (**33**, *TTC*₁ and **35**, *TTC*₂) characterized by rotation of the pyran fragment.

Thus, thermal ring opening of the NO₂-containing SPOD proceeds along a complex pathway shown in Fig. 7. Besides two main TSs **28** and **32** defining the energetics of the process under consideration and being present on the ring opening pathway of SPPs and SPOs, low-energy transition structures **30** (**TS**_{*CTC*}) and **34** (**TS**_{*TTC*}) were detected between isomers **29**, *CTC*₁ and **31**, *CTC*₂, as well as between **33**, *TTC*₁ and **35**, *TTC*₂ with a transoid configuration.

Table 3. DFT/B3LYP/6-311++G(d,p)-calculated relative energies without (ΔE) and with taking into account the zero-point harmonic vibration energies (ΔE_{ZPE}) for structures **27**–**37**

Structure	ΔE	ΔE_{ZPE}
	kcal mol ⁻¹	
27 , <i>Closed</i>	1.5	2.5
28 , <i>TS</i> ₁	13.9	13.7
29 , <i>CTC</i> ₁	4.1	3.9
30 , <i>TS</i> _{<i>CTC</i>}	6.8	6.4
31 , <i>CTC</i> ₂	4.1	3.9
32 , <i>TS</i> ₂	10.9	10.0
33 , <i>TTC</i> ₁	2.2	2.0
34 , <i>TS</i> _{<i>TTC</i>}	2.5	2.3
35 , <i>TTC</i> ₂	2.2	2.0
36 , <i>TTT</i>	0.0	0.0
37 , <i>CTT</i>	2.1	2.0

Note. The corresponding absolute total energies (au) for structure **36** are $E_{\text{tot}} = -1102.27577$ and $E_{\text{tot, ZPE}} = -1101.96752$.

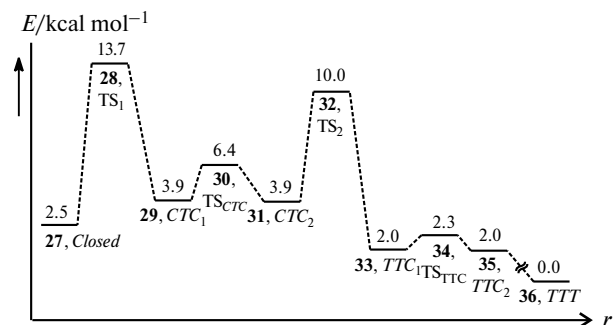


Fig. 7. Energy diagram for thermal ring opening of the NO₂-containing SPOD according to the DFT/B3LYP/6-311++G(d,p) calculation data.

The photochromic properties of SPPs and SPOs are caused by the absence of absorption in the visible spectral region in the closed forms and by the presence of electron transitions in this range in the open forms.^{1,3,4} TD DFT (B3LYP/6-311++G(d,p)) calculation of the electronic spectrum of the SPOD closed form **18** predicts the existence of two absorptions bands in the range from 400 to 500 nm (at 460 and 427 nm) (Fig. 8).

Consideration of the nonspecific solvation (acetonitrile) results in a slight shift of these electron transitions compared to the gas phase and an increase in the intensity of the long-wavelength band (see Fig. 8, b). The spectrum of the most stable ring-opened *TTT* form **24** of SPOD is predicted to contain a band with a maximum at 460 nm which shifts up to 493 nm when taking into account the solvent effect. The closeness between the absorption band

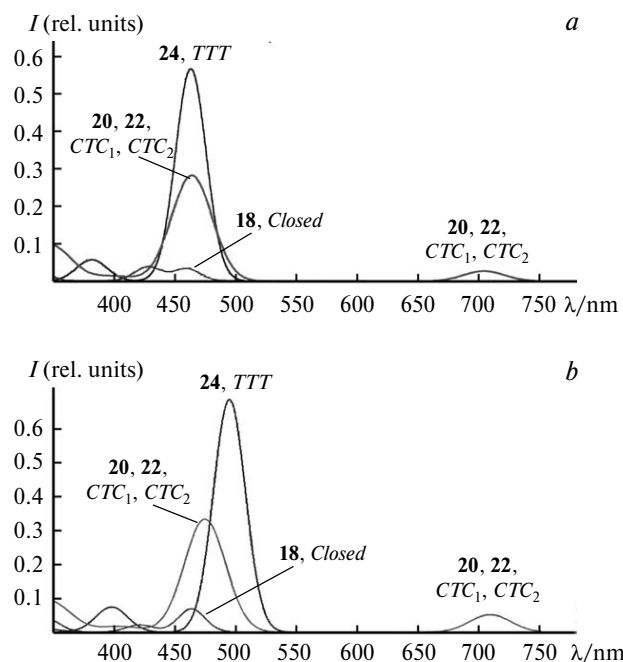


Fig. 8. TD DFT (B3LYP/6-311++G(d,p))-calculated electronic spectra of structures **18**, **20**, **22**, and **24** without (a) and with taking into account the nonspecific solvation (b) (IEFPCM, MeCN).

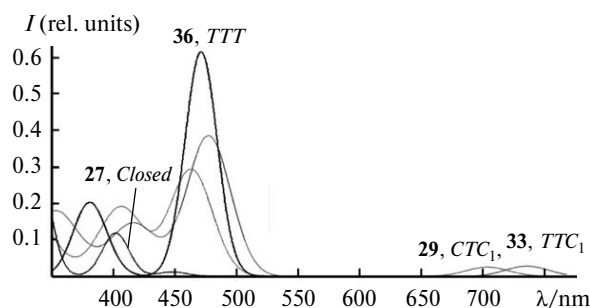


Fig. 9. TD DFT (B3LYP/6-311++G(d,p))-calculated electronic spectra of structures **27**, **29**, **33**, and **36**.

maxima of the ring-closed (**18**) and ring-opened (**24**) forms of SPOD suggests a low probability of photoinitiated ring opening—closure, since light irradiation will have simultaneous effect on both forms of the compound.

The spectra of the CTC isomers **20** and **22** characterized by rotation of the pyran fragment relative to the indoline one contain long-wavelength transitions at ~ 700 nm (see Fig. 8, *a*). The analogous transitions at ~ 550 nm are predicted for the planar structures **24–26** (TTT, CTT, and TTC); however, their intensities are almost zero. As it follows from calculations of the electronic spectrum of SPOD with the NO₂-substituted indoline fragment, the electron-withdrawing substituent has an insignificant effect on the electron transitions in the ring-opened forms, which results in a decrease in the long-wavelength band intensity of the closed form (Fig. 9).

Thus, the performed quantum chemical study suggests that the cyclic forms of SPODs are energetically unfavorable compared to the open merocyanine form whose ground state corresponds to the TTT isomers. It is this fact which is likely the reason for the disinterest in SPODs as compounds with possible photochemical behavior. Another significant feature of compounds of this type distinguishing them from the analogs (SPPs and SPOs) is the mechanism of oxadiazine ring opening—closure, *i.e.*, a nonrealizability of the CCC isomer caused by the stereochemical nonrigidity of the N—N fragment. The study of the mechanism of SPOD isomerization showed that the process requires low energy costs (~ 10 kcal mol⁻¹). Different conformations of the open isomers are characterized by close energies, which must result in their coexistence in solution. The presence of long-wavelength transitions in the closed forms of SPODs virtually coinciding with the transitions predicted for the open forms complicates the photochemistry of SPODs and imposes constraints on the applicability of these compounds as photochromic switches.

This work was financially supported by the Ministry of Education and Science of the Russian Federation as a part of the State Task (Project No. 1895).

References

1. *Molecular Switches*, Eds B. L. Feringa, W. R. Browne, Vol. 1–2, Wiley-VCH, Weinheim, Germany, 2011.
2. V. I. Minkin, *Russ. Chem. Bull. (Int. Ed.)*, 2008, **57**, 687 [*Izv. Akad. Nauk, Ser. Khim.*, 2008, 673].
3. *Techniques of Chemistry*, Vol. III: *Photochromism*, Ed. G. H. Brown, Wiley-Interscience, New York, 1971, 853 pp.
4. *Photochromism. Molecules and Systems*, Eds H. Dürr, H. Bouas-Laurent, Elsevier, Amsterdam, 1990, 1044 pp.
5. *Organic Photochromic and Thermochromic Compounds*, Eds J. C. Crano, R. J. Guglielmetti, Vol. 1–2, Plenum Press, New York, 2000.
6. G. Bercovic, V. Krongauz, V. Weiss, *Chem. Rev.*, 2000, **100**, 1741.
7. V. Lokshin, A. Samat, A. V. Metelitsa, *Russ. Chem. Rev.*, 2002, **71**, 893.
8. V. I. Minkin, *Chem. Rev.*, 2004, **104**, 2751.
9. V. I. Minkin, *Russ. Chem. Rev.*, 2013, **82**, 1.
10. R. Klajn, *Chem. Soc. Rev.*, 2014, **43**, 148.
11. M. J. Frisch, G. W. Trucks, H. B. Schlegel, G. E. Scuseria, M. A. Robb, J. R. Cheeseman, J. A. Montgomery, Jr., T. Vreven, K. N. Kudin, J. C. Burant, J. M. Millam, S. S. Iyengar, J. Tomasi, V. Barone, B. Mennucci, M. Cossi, G. Scalmani, N. Rega, G. A. Petersson, H. Nakatsuji, M. Hada, M. Ehara, K. Toyota, R. Fukuda, J. Hasegawa, M. Ishida, T. Nakajima, Y. Honda, O. Kitao, H. Nakai, M. Klene, X. Li, J. E. Knox, H. P. Hratchian, J. B. Cross, V. Bakken, C. Adamo, J. Jaramillo, R. Gomperts, R. E. Stratmann, O. Yazyev, A. J. Austin, R. Cammi, C. Pomelli, J. W. Ochterski, P. Y. Ayala, K. Morokuma, G. A. Voth, P. Salvador, J. J. Dannenberg, V. G. Zakrzewski, S. Dapprich, A. D. Daniels, M. C. Strain, O. Farkas, D. K. Malick, A. D. Rabuck, K. Raghavachari, J. B. Foresman, J. V. Ortiz, Q. Cui, A. G. Baboul, S. Clifford, J. Cioslowski, B. B. Stefanov, G. Liu, A. Liashenko, P. Piskorz, I. Komaromi, R. L. Martin, D. J. Fox, T. Keith, M. A. Al-Laham, C. Y. Peng, A. Nanayakkara, M. Challacombe, P. M. W. Gill, B. Johnson, W. Chen, M. W. Wong, C. Gonzalez, J. A. Pople, *GAUSSIAN 03, Revision E.01*, Gaussian, Inc., Wallingford (CT), 2004.
12. W. Kohn, L. J. Sham, *Phys. Rev.*, 1965, **140**, A1133.
13. A. D. J. Becke, *J. Chem. Phys.*, 1993, **98**, 5648.
14. V. I. Minkin, A. G. Starikov, R. M. Minyaev, A. A. Starikova, *Theor. Exp. Chem. (Engl. Transl.)*, 2011, **46**, 363 [*Teor. Eksperim. Khim.*, 2010, **46**, 352].
15. A. A. Starikova, R. M. Minyaev, A. G. Starikov, V. I. Minkin, *Dokl. Chem. (Engl. Transl.)*, 2013, **453**, 263 [*Dokl. Akad. Nauk Khim.*, 2013, **453**, 401].
16. A. A. Starikova, R. M. Minyaev, A. G. Starikov, V. I. Minkin, *Eur. J. Inorg. Chem.*, 2013, 4203.
17. R. M. Minyaev, *Russ. Chem. Rev.*, 1994, **63**, 883.
18. V. Barone, M. Cossi, *J. Phys. Chem. A*, 1998, **102**, 1995.
19. *Chemcraft, version 1.7*, 2013: <http://www.chemcraftprog.com>.
20. S. Nakamura, K. Uchida, A. Murakami, M. Irie, *J. Org. Chem.*, 1993, **58**, 5543.
21. T. Horii, Y. Abe, R. Nakao, *J. Photochem. Photobiol. A*, 2001, **144**, 119.
22. V. I. Minkin, A. V. Metelitsa, I. V. Dorogan, B. S. Lukyanov, S. O. Besugliy, J.-C. Micheau, *J. Phys. Chem. A*, 2005, **109**, 9605.
23. F. Maurel, J. Aubard, M. Rajzmann, R. Guglielmetti, A. Samat, *J. Chem. Soc., Perkin Trans. 2*, 2002, 1307.
24. A. Perrier, F. Maurel, E. A. Perpète, V. Wathélet, D. Jacquemin, *J. Phys. Chem. A*, 2009, **113**, 13004.

Received April 30, 2015;
in revised form July 31, 2015